



Contents lists available at ScienceDirect

Journal of Advanced Research

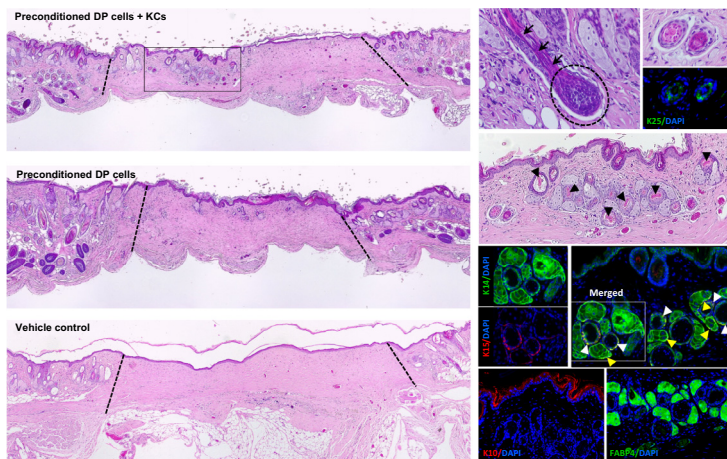
journal homepage: www.elsevier.com/locate/jare

Rescuing key native traits in cultured dermal papilla cells for human hair regeneration

Carla M. Abreu, Mariana T. Cerqueira, Rogério P. Pirraco, Luca Gasperini, Rui L. Reis, Alexandra P. Marques*

3B's Research Group – Biomaterials, Biodegradables and Biomimetics, Headquarters of the European Institute of Excellence on Tissue Engineering and Regenerative Medicine, University of Minho, Avepark 4805-017 Barco, Guimarães, Portugal
ICVS/3B's – PT Government Associate Laboratory, Braga/Guimarães, Portugal

GRAPHICAL ABSTRACT



ARTICLE INFO

Article history:
Received 14 September 2020
Revised 22 October 2020
Accepted 29 October 2020
Available online xxxx

Keywords:
Hair follicle
Dermal papilla cells
Keratinocyte-conditioned medium
Hair inductivity
Hair follicle regeneration

ABSTRACT

Background: The dermal papilla (DP) represents the major regulatory entity within the hair follicle (HF), inducing hair formation and growth through reciprocal interactions with epithelial cells. However, human DP cells rapidly lose their hair inductive ability when removed from their niche and cultured in an epithelium-deficient environment.

Methods: Conditioned medium collected from interfollicular keratinocytes (KCs-CM) was used to culture DP cells both in 2D and 3D culture conditions and investigate how it impacts the native properties and inductive phenotype of these cells. Further, the hair-inductive capacity of DP cells precultured with KCs-CM was tested in a hair reconstitution assay, after co-grafting with human keratinocytes in nude mice. **Results:** We demonstrate that KCs-CM contributes to restore the inductivity of cultured human DP cells in a more effective mode than the conventional 3D-cultures. This is supported by the higher active alkaline phosphatase (ALP) levels in DP cells, the improved self-aggregative capacity and the reduced expression of α -SMA and the V1-isoform of versican. Moreover, DP cells cultured with KCs-CM displayed a secretome profile (VEGF, BMP2, TGF- β 1, IL-6) that matches the one observed during anagen. KCs-CM also enhanced DP cell proliferation, while preventing cells to undergo morphological changes characteristic of high passage cells. In opposition, the amount of collagenous and non-collagenous proteins deposited by

Peer review under responsibility of Cairo University.

* Corresponding author at: 3B's Research Group.

E-mail address: apmarques@i3bs.uminho.pt (A.P. Marques).

<https://doi.org/10.1016/j.jare.2020.10.006>

2090-1232/© 2020 THE AUTHORS. Published by Elsevier BV on behalf of Cairo University.

This is an open access article under the CC BY-NC-ND license (<http://creativecommons.org/licenses/by-nc-nd/4.0/>).

DP cells was lower in the presence of KCs-CM. The improvement in ALP activity was maintained in 3D spheroidal cultures, even after KCs-CM retrieval, being superior to the effect of the gold-standard culture conditions. Moreover, DP cells cultured with KCs-CM and grafted with human keratinocytes supported the formation of HF- and sebaceous gland-like structures in mice.

Conclusion: The proposed strategy encourages future cell-based strategies for HF regeneration not only in the context of hair-associated disorders, but also in the management of wounds to aid in restoring critical skin regulatory appendages.

© 2020 THE AUTHORS. Published by Elsevier BV on behalf of Cairo University. This is an open access article under the CC BY-NC-ND license (<http://creativecommons.org/licenses/by-nc-nd/4.0/>).

Introduction

The dermal papilla (DP) is the key mesenchymal compartment involved in hair growth. It is organized as a cluster of highly specialized cells located at the base of the hair follicle (HF), a privileged position from where the DP activates and controls hair growth, through reciprocal interactions with the neighbouring epithelium [1–3]. The use of DP cells for HF regenerative approaches relies both on their propagation and in the maintenance of their inductive properties in culture, to ensure that a proper number of functional cells is obtained. However, the quick loss of inductivity that human DP cells experience in culture [4], and from which they don't spontaneously recover, has been hindering the development of DP cell-based strategies for HF regeneration. So far, the most efficient method to restore human DP cell inductivity is the artificial recreation of the cells' 3D architecture and intercellular contacts using 3D spheroid cultures [4,5]. While it results in a partial recovery of human DP cell transcriptome [4] and native signature [5] *in vitro*, the hair-induction rate of DP spheroids in a human-to-human recombinant assay was only of 15% [4]. This illustrates the difficulty in regenerating human hairs, as well as the need to further develop new approaches to improve the inductive properties of human DP cells.

Strategies capable of addressing that need include the stimulation of the Wnt/ β -catenin, BMP and FGF signalling pathways in culture DP cells using specific targeting biomolecules [6,7]. However, the obtained cells still failed to form hairs *in vivo* [7]. More recently, Won *et al* [8] reported that the use of concentrated conditioned medium (CM) collected from human $\alpha 6$ -integrin^{high}/CD71^{low} keratinocytes (KCs) has a hair growth-promoting effect in mice. The CM contained different growth factors, including vascular endothelial growth factor (VEGF) and platelet-derived growth factor-A (PDGF-A), among others. The topical injection of these factors in telogen-synchronized mice replicated the CM effect confirming improved hair growth due to an earlier telogen-to-anagen transition. This study supports what has been previously shown regarding the importance of epithelial-mesenchymal interactions (EMIs) for hair growth promotion [9]. But whether the recreation of this complex epithelial signalling *in vitro* is beneficial towards the recovery of the inductive phenotype of human DP cells, and ultimately hair regeneration is yet to be demonstrated. Studies with co-culture systems using human cells [10–12] did not investigate epithelial cell effects on DP cells. In turn, KCs-CM was shown to improve human DP cell proliferation [8,13], but its impact on the hair inductive-associated phenotype or trichogenic ability was not addressed. Considering this, we hypothesised that by culturing human DP cells with KCs-CM some of the epithelial-mesenchymal interactions would be recreated, promoting the restoration of an inductive phenotype, while simultaneously supporting their proliferation. We uncover the effects of KCs-CM in the recovery of DP cell inductive properties and native phenotype under the standard 2D culture conditions used for their expansion. The persistence of the effect over DP cell inductivity *in vitro* was further demonstrated in 3D cultures even after

KCs-CM stimulus withdrawal, which is determinant to maximise DP cell effectiveness in long term. We propose an efficient and simple approach to attain human DP cells with an improved phenotype and capable of inducing the formation of HF-like structures.

Materials and methods

Ethics statement

All the experimental protocols involving animals were approved by the local animal welfare body (ethical approval no. ORBEA EM/ICVS-I3Bs_009/2019) and performed according to the applicable national regulations and international animal welfare rules. Human tissue samples were obtained after informed consent from the patients and under a collaboration protocol approved by the ethic committees of the involved institutions (approval no. 05 CEASS|SCMP, study no. 005/2019).

Cell isolation and culture

J2-3 T3 fibroblasts were cultured in DMEM supplemented with 10% adult bovine serum, up to passage 10. Feeders were prepared with 2.4×10^4 cells/cm² after inhibition with mitomycin C (4 μ g/ml) for 2 h 30 min at 37 °C. KCs were isolated from human skin tissue obtained from patients who underwent abdominoplasty surgery in Hospital da Prelada (Porto, Portugal), as previously described [14], and cultured in Keratinocyte Serum-free Medium (KFSM, Gibco) with Y-27632 (10 μ M; STEMCELL Technologies). KCs were resuspended in FAD medium [DMEM/Ham's F12 medium (3:1 ratio) supplemented with 1.8×10^{-4} M adenine, 10% non-inactivated fetal bovine serum (FBS), 0.5 μ g/ml hydrocortisone, 10^{-10} M cholera toxin, 10 ng/ml epidermal growth factor, 5 μ g/ml insulin and 1.8 mM CaCl₂]. Scalp samples were obtained from hair transplantation surgeries performed at Sanare - Unicapilar Clínica (Porto, Portugal) and used to isolate DP cells by the standard microdissection technique [15]. Explants were initially cultured in DMEM 20% FBS. After passage, DP cells were cultured in DMEM 10% FBS and used from passage 4 to 6. All cells were cultured in a humidified incubator at 37 °C and 5% CO₂, with medium changes every 2–3 days.

KCs-CM collection and usage in DP cell cultures

Keratinocytes (1.0 – 1.4×10^5) at passage 1 were seeded in 75 cm² flask previously prepared with feeder cells. Approximately after one week, KCs were removed from the feeder layer and 2.5×10^6 cells were cultured in 150 cm² culture flasks with 20 mL of KFSM with Y-27632. CM was collected at day 6 of culture, after a medium change at day 4. The collected supernatant was filtered through a 0.22 μ m syringe filter and stored at –20 °C until further use, up to one month. DP cells were cultured in DMEM with 10% FBS overnight. In the following day, the medium was replaced by the collected CM mixed with an equal volume of fresh DMEM

10% FBS (KCs-CM). DP cells cultured in their standard medium - DMEM 10% FBS - (DMEM), or in DMEM mixed with an equal volume of KSMF with Y-27632 - (Medium CTRL) were prepared as controls. Culture medium was refreshed every two days, up to 5 days.

DNA and active-alkaline phosphatase (ALP) quantification

DP cells were lysed with ultra-pure water with 0.01% sodium dodecyl sulphate (1 h, 37 °C), followed by freezing at -80 °C. Cells were then scrapped, and DNA levels quantified using the PicoGreen™ dsDNA Assay Kit (Thermo Fisher Scientific) and the amount of active-ALP was quantified using the Alkaline Phosphatase Detection Kit (Sigma-Aldrich).

Detection of ALP-active cells

Adherent cells were fixed in 10%-formalin (15 mins, RT) and the nitro-blue tetrazolium chloride and 5-bromo-4-chloro-3'-indoly phosphate (NBT/BCIP) substrate was prepared by diluting 5 µL of NBT and 3.75 µL of BCIP (Roche) per mL of staining buffer (100 mM NaCl, 100 mM Tris-HCl pH 9.5 and 50 mM MgCl₂ in water). The substrate was applied for 20 min (RT, dark) and washed with water before observation.

Immunocytochemistry

Fixed DP cells were permeabilized with 0.2% Triton X-100 for 15 min at RT (in case of intracellular staining) or with 1% Triton X-100 for 30 min on ice (in case of nuclear staining), and incubated with 3% bovine serum albumin (BSA, Sigma-Aldrich) in PBS for 45 min (RT) to block nonspecific staining. Primary antibodies (Supplementary Table 2) were diluted in 1% BSA solution containing 0.2% Triton X-100 and incubated for 1 h (RT). Samples were then washed with PBS and incubated with Alexa Fluor (AF) (488/594)-conjugated secondary antibodies (1:500; Molecular Probes) prepared in the same conditions as primary antibodies. Cell's F-actin fibers were stained with phalloidin-TRITC (1:100, Sigma-Aldrich) and nuclei with 4',6'-diamino-2-phenylindole (DAPI) (0.02 mg/mL; Biotium). Samples were analysed and images acquired with an Axioplan Imager Z1m microscope (Zeiss).

Flow cytometry

For cell surface marker analysis, DP cells were resuspended in DMEM 10% FBS and incubated with the CD184-APC (1:20; BioLegend) or the LRP4-PE (1:10; Miltenyi Biotec) antibodies respectively for 30 min (RT) or 10 min (ice). For intracellular staining, the FIX & PERM™ Cell Permeabilization Kit (Thermo Fisher Scientific) was used. Cells were first fixed with reagent A (15 min, RT), washed in PBS, then permeabilized with reagent B and incubated (20 min, RT) with the α -SMA-FITC (1:33; Abcam) or LEF1-AF488 (1:50; Cell Signaling Technology) antibodies. Cell suspensions were analysed with a FACSCalibur flow cytometer (BD Biosciences) using the Cell Quest Software for data analysis.

Collagen and non-collagenous proteins staining and quantification

The production of collagenous (COL) and non-collagenous (NCOL) proteins by DP cells was measured using the Sirius Red/Fast Green Collagen Staining Kit (Chondrex Inc.). Formalin-fixed cells were immersed in the dye solution (30 min, RT) and washed in water until it runs clear. Representative images were acquired with a Leica DM750 microscope (Leica). Further quantification was performed by extracting the dye with the kit destaining solution and measuring the samples optical density at 540 nm (Sirius

red, COL proteins) and 605 nm (fast green, NCOL proteins). The colour equivalences [16] were used to calculate the quantity of COL and NCOL proteins produced.

Glycosaminoglycans staining and quantification

Fixed cells were rinsed in 3% acetic acid and further stained with 1% Alcian Blue (pH 2.5, Sigma-Aldrich) for 30 min at RT. After washing in water, the presence of GAGs was examined, and representative images were acquired. Sulphated GAGs production was quantified using the 1,9-dimethylmethylene blue (DMMB) assay [17]. Briefly, DP cells were digested at 60 °C (overnight) in a 0.05% of papain and 0.096% of N-acetyl cysteine solution prepared in 200 mM of phosphate buffer with 1 mM EDTA (pH 6.8). Samples were then centrifuged (13000 rpm, 10 min) and the supernatants incubated with 250 µL of DMMB solution (16 mg DMMB in 1 L water containing 3.04 g glycine and 1.6 g NaCl, pH 3.0). Optical density at 530 nm was read using a microplate reader (Synergy HT, BioTek), and DMMB-GAGs complexes amount was extrapolated using a chondroitin sulphate standard curve.

ELISA

After 5 days in culture, DP cell medium was replaced by the equivalent FBS-free media and cultured for 24 h. The supernatant was then collected, centrifuged (3000 rpm, 10 min) and stored at -80 °C in single-use aliquots. VEGF ELISA Development Kit, BMP2 Standard ELISA Development Kit (Peprotech), PDGF-AA DuoSet ELISA, IL-6 DuoSet ELISA (R&D Systems) and TGF- β 1 Elisa kit (Invitrogen) were used according to the manufacturer's instructions. Control wells with FBS-free media incubated in the same conditions but without cells were used to determine the amount of each biomolecule in the different media used.

Self-aggregation assay

Fixed cells were washed in PBS and incubated with DAPI for 15 min at RT. The nuclei were visualized under a Zeiss Axio Observer microscope and 10 pictures/triplicate were taken at different fields. Nuclei staining was used to assess DP cell aggregation using the CellProfiler™ 3.0.0 [18]. Images were first converted to grey-scale, and the nuclei signal identified by applying Otsu thresholding algorithm [19] to differentiate signal from background. Cells were regarded as adjacent if the distance between their nuclei was below 8 pixels. Groups of 50 or more adjacent cells were considered an aggregate.

Spheroid formation assay

After culture with KCs-CM, 1×10^4 DP cells were seeded in round bottom ultra-low attachment 96-well plates (Corning), whereas DP cells cultured in DMEM or Medium CTRL were used as controls. Cells were cultured in the respective culture medium, under standard culture conditions (37 °C, 5% CO₂), and time-lapse microscopy (Axio Observer, Zeiss) was used to record spheroid formation in the centre of the well. The 2D-area occupied by the cells was quantified at different time points using the ZEN 2 software (Zeiss).

3D spheroid culture and analysis

DP cells precultured in KCs-CM were seeded in round bottom ultra-low attachment 96-well plates at a density of 5×10^3 cells/mL, and cultured in 50 µL DMEM 10% FBS. DP cells precultured in control media (DMEM or Medium CTRL) were also used as controls. Upon 4 days of culture, the spheroids were washed in PBS and collected. The quantification of DNA and the amount of

active-ALP were performed as described. A 5 s sonication step in ice was performed to guarantee the complete disintegration of the spheroid prior quantification. The same cell lysates were used for total protein quantification, using a Bradford-based Protein Dye (BioRad). Briefly, samples were diluted in water with 0.01% Triton X-100, and 4-parts of the diluted sample were added with 1-part of dye reagent. The absorbance was read at 595 nm and protein content was interpolated against a BSA-standard curve.

Hair reconstitution assay

6-mm full-thickness wounds were made on the back of immunodeficient nude mice (athymic Nude-Foxn1tm, Charles River) and silicon chambers were inserted under the skin (one chamber per animal) [20]. A mixture of 5.0×10^6 CM-precultured DP cells and 2.5×10^6 KCs were injected into the chamber. Cell suspensions of 5×10^6 CM-precultured DP cells or vehicle (FAD medium) were injected as controls. The top of the silicon chambers was cut off after 1 week and the chamber was completely removed 2 weeks after the injection of the cells. The animals were euthanized 6 weeks after surgery and the wound area and surrounding tissue were collected for histological analysis.

Histological and immunological stainings

Paraffin-embedded sections of 4- μ m (*in vivo* samples) or 10- μ m (spheroids) were dewaxed in xylene, rehydrated and heat-mediated antigen retrieval (sodium citrate buffer, pH 6.0) was performed before starting the immunolabelling procedure, as previously described in the "Immunocytochemistry" section. For primary antibodies (Supplementary Table 2) raised on mice, a mouse-on-mouse kit (Vector Laboratories) was used to block background caused by endogenous mouse Ig. Sections stained with Haematoxylin & Eosin (H&E) were analysed with a Leica DM750 microscope while the remaining specimens were analysed with an Axio Imager Z1m microscope (Zeiss).

In situ hybridization

The presence of human cells within the wound area was assessed using the human-specific DNA oligo probe of the BIO-HRP REMBRANDT[®] Universal DISH detection kit (PanPath). Briefly, unspecific staining in dewaxed sections was blocked with a 3% solution of hydrogen peroxide (15 min, RT). Proteolytic digestion was then performed using a pepsin-HCL solution for 30 min at 37 °C, followed by dehydration in graded ethanol solutions. Samples were then air-dried and 1 drop of the probe was applied and covered with a coverslip. DNA denaturation was performed at 95 °C for 5 min, and hybridization was let to occur for 16 h at 37 °C in a moisturized environment. Samples were then washed in tris-buffered saline (TBS) and incubated for 10 min with the stringency wash buffer. After rinsing with TBS, the detection was performed using the kit AEC substrate detection system. Colour was let to develop for 10 min at 37 °C (dark). Samples were washed with water and observed under a DM750 light microscope (Leica).

Statistical analysis

Experiments were performed using DP cells isolated from three donors and CM variability was ensured by collection from KCs isolated from six donors. When the number of independent experiments was higher than 3, the KCs-CM from cells isolated from 6 different donors was tested with DP cells from the 3 different donors in different combinations. The statistical analysis was performed using the GraphPad Prism 7.03 software. To test if data followed a Gaussian distribution, the D'Agostino & Pearson normality

test was used. Nonparametric data were analysed with a Kruskal-Wallis (unpaired) or a Friedman test (paired), both coupled with Dunn's post-test. For results that did follow a Gaussian distribution, RM one-way ANOVA (paired) or ordinary one-way ANOVA (unpaired) were used in combination with Tukey's post-test. For data where two independent variables were considered, a two-way ANOVA was used (paired) followed by Tukey's post-test. Results are expressed as mean \pm s.e.m and differences with *p*-values < 0.05 were set as significant.

Results

Improvement of DP cell inductive phenotype by KCs-CM

When deprived of their native milieu and cultured in plain 2D culture conditions, DP cells suffer a rapid loss of their inductive potency [4]. To understand if KCs-CM could restore determinant functional features of DP cells in culture, we assessed the amount of active ALP, and the expression of α -SMA and versican, all known markers for DP cells [1]. *In situ*, DP cells do not express α -SMA and the V2-isoform of versican is predominantly expressed, whereas *in vitro* α -SMA and the V1-isoform become widely expressed [21,22]. After culture in KCs-CM a significant increase of active ALP (Fig. 1a,b), together with a significant reduction in the expression of α -SMA (Fig. 1c,d) and the V1-isoform of versican (Fig. 1d) were observed compared to standard DP cell expansion conditions (DMEM). Although KCs-CM did not restore the expression of the V2-isoform of versican (Fig. 1d), it is evident that it supports a partial recovery of important markers of DP cell phenotype.

To test if KCs-CM also impacts DP cell self-aggregative behaviour, which is negatively affected in 2D cultures [4], we studied cellular aggregation. The number of cell aggregates was significantly higher when DP cells were culture with KCs-CM in comparison to the control groups (Fig. 1e,f). Further, we analysed the kinetics of DP cell aggregation when cultured in round-bottom plates (Supplementary Video). DP cell aggregates were formed earlier and were more compact in the presence of KCs-CM than in controls (Fig. 1g,h), suggesting a positive effect of KCs-CM in the recovery of DP cell self-aggregation capacity.

During anagen, the hair cycle phase where DP inductivity is higher [23], the production of the angiogenic factor VEGF is necessary for the development of a capillary network within the HF dermal compartment [24,25] and for the promotion of hair growth [26]. Similarly, IL-6 is a multifactorial cytokine strongly expressed in the HF during anagen [27] and known to regulate KCs proliferation and differentiation [28]. In turn, BMP molecules [29] and TGF- β 1 [30] are downregulated for anagen onset, to avoid KCs differentiation and even apoptosis. PDGF-A is also known to induce and maintains anagen [31] and to have hair growth-inducing capacity [32]. Considering this signalling network, we investigated if KCs-CM could affect the secretion of these paracrine mediators of hair growth by DP cells. DP cells cultured in KCs-CM secreted significantly more VEGF (Fig. 1i), albeit about one-third of this amount could be attributed to KCs-CM (Supplementary Fig. 1a). In what concerns BMP2 (Fig. 1j) and TGF- β 1 (Fig. 1k) secretion, a significant decrease was observed in cultures with KCs-CM. However, the level of TGF- β 1 in the KCs-CM condition and control medium was similar, which seems to indicate that DP cells were responding to the culture medium and not to KCs-CM. In contrast, BMP2 secretion did not vary among controls, suggesting that the effect observed in the experimental group was mostly related to KCs-CM. Both factors were absent in KCs-CM (Supplementary Fig. 1a). The most striking effect of CM treatment was an almost 223-fold increase in the amount of IL-6 (Fig. 1l), which was undetectable in KCs-CM and was present in low amounts in control conditions. PDGF-A was not detected in cultures with KCs-CM (Supplementary

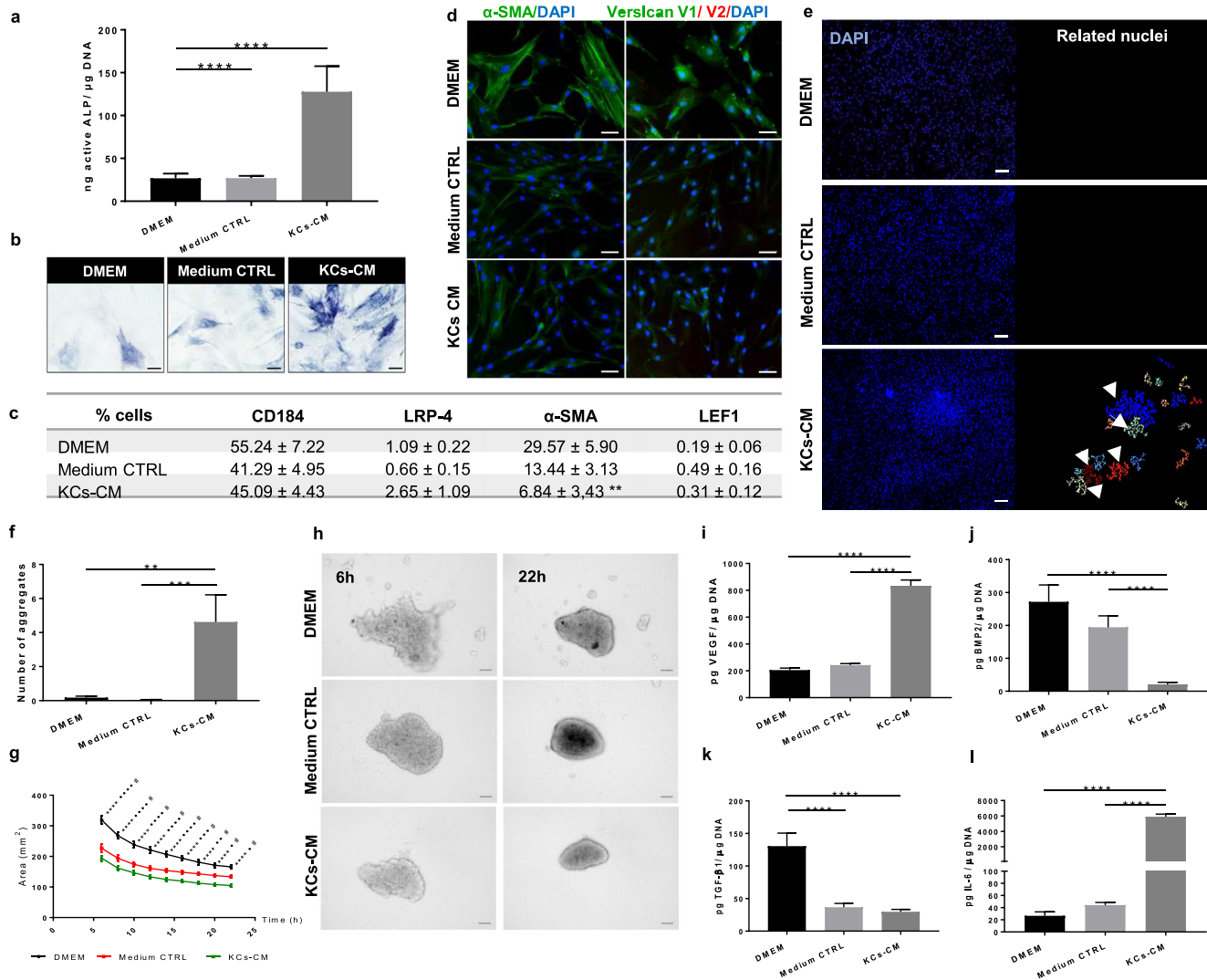


Fig. 1. KCs-CM improves DP cell inductive phenotype. **(a)** Amount of active ALP and **(b)** respective images of ALP-active DP cells showing an improvement of the DP cell inductive-related phenotype after culture with KCs-CM ($n = 6$). **(c)** Percentage of DP cells expressing CD184, LRP-4, α -SMA ($n = 7$) and LEF1 determined by flow cytometry ($n = 5$, ** $p < 0.01$ vs DMEM). **(d)** Expression of α -SMA and the V1-isoform of versican in DP cells confirming a decrease after culture with KCs-CM. **(e)** Representative DAPI-stained nuclei images used to perform image analysis and **(f)** quantify the number of DP cell aggregates formed after 5 days in culture showing that DP cells treated with KCs-CM have improved capacity to self-aggregate ($n = 3$) **(g)** Variation of the area occupied by the DP cells up to 22 h of culture as obtained by the **(h)** analysis of time-lapse images showing that DP cells cultured in KCs-CM form more compact spheroids and faster than controls ($n = 6$). **(i-k)** Amount of growth factors and **(l)** cytokine secreted by DP cells showing the difference of their secretome with the culture conditions. Data shown are mean \pm s.e.m. Differences are indicated by * KCs-CM vs DMEM, # KCs-CM vs Medium CTRL and • Medium CTRL vs DMEM. * $p < 0.05$; ** $p < 0.01$; *** $p < 0.001$; **** $p < 0.0001$. Scale bars are 50 μ m for **(b,d)**, 100 μ m for **(h)** and 200 μ m for **(e)**.

Fig. 1b), even though it was present in the KCs-CM itself (**Supplementary Fig. 1a**). Our findings demonstrate that KCs-CM can modulate DP cell secretome to match in some extent the signalling environment during anagen.

KCs-CM improves DP cell proliferation but decreases matrix deposition ability

Another factor preventing the attainment of high numbers of functional DP cells is their low proliferative capacity, probably reminiscent of their quiescent state *in situ*, where <2% of the cells are proliferative [5,33]. Moreover, DP cells relatively short lifespan in culture [34] further restricts the number of healthy cells obtained. Considering this, we demonstrated that KCs-CM can promote DP cell expansion, as shown by the significantly higher cell number (**Fig. 2a**). Further, DP cells cultured in KCs-CM showed a spindle-like shape in opposition to the flat enlarged morphology

characteristic of higher passaged cells [35] and observed in standard DP expansion conditions (**Fig. 2b**).

The DP is a densely packed cellular structure surrounded by an extracellular matrix (ECM) comprising mostly fibronectin, laminin, collagen IV and sulphated glycosaminoglycans (GAGs), and lower collagen I content [36,37]. Culturing DP cells in the presence of KCs-CM led to a significantly lower capacity to deposit both COL and NCOL proteins (**Fig. 2c,d,e**). The COL/NCOL ratio was also significantly lower for CM-cultured DP cells in comparison to standard DMEM culture (**Fig. 2f**). The expression of proteins analysed by immunocytochemistry, seemed to confirm a dimmed signal for DP cells cultured in KCs-CM in comparison to controls (**Fig. 2g**). Moreover, collagen I appeared to be less expressed than fibronectin (**Fig. 2g**), while the deposition of collagen IV was not detected (data not shown). KCs-CM also negatively affected the deposition of GAGs, which is reflected in the amount of sulfated GAGs produced (**Fig. 2h**), as well as in their distribution pattern within the whole ECM (**Fig. 2i**).

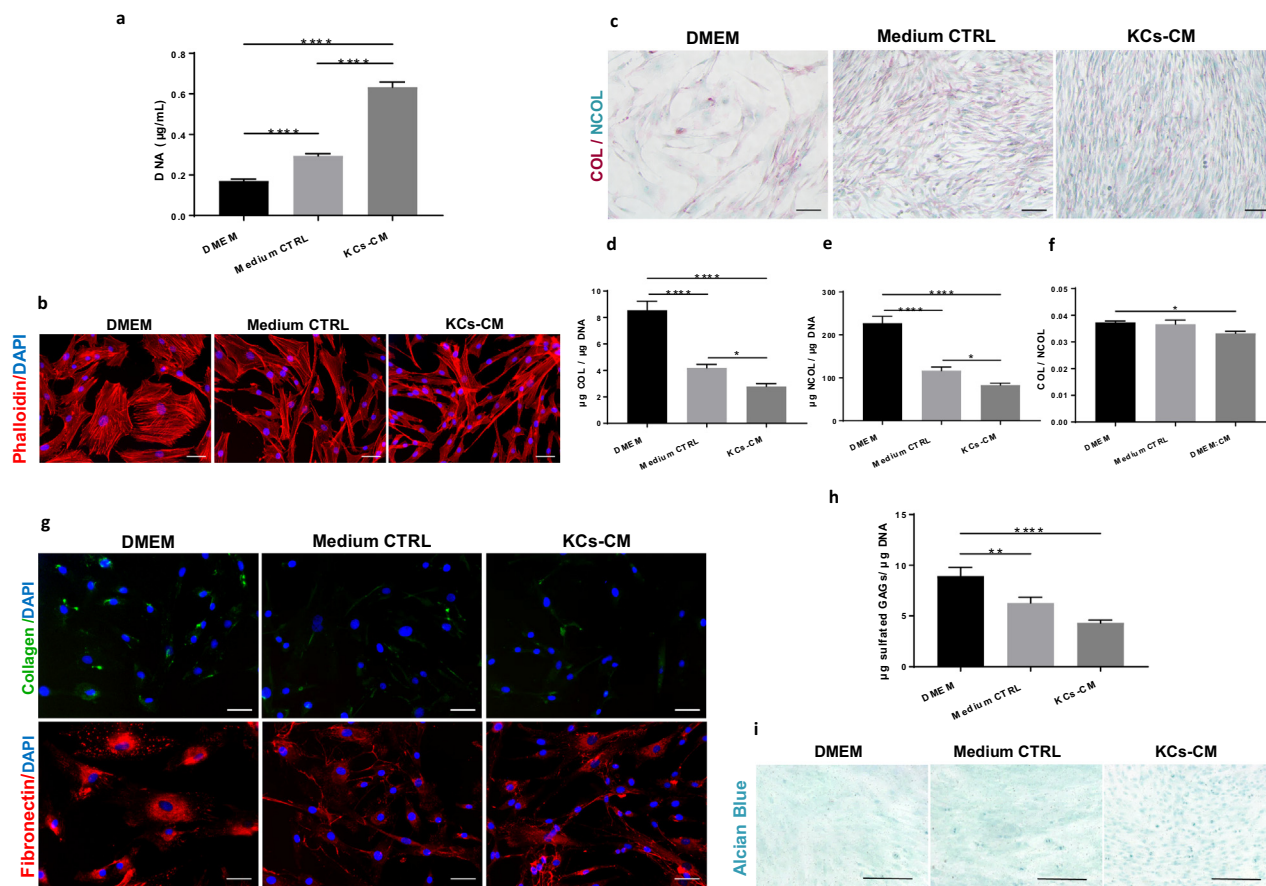


Fig. 2. KCs-CM beneficially affect DP cells proliferation but decreases matrix deposition ability. **(a)** DNA levels demonstrating that KCs-CM increases DP cell numbers ($n = 9$). **(b)** Phalloidin-TRITC stained F-actin cytoskeleton showing that CM-treatment prevents an enlarged morphology in DP cells. **(c)** Representative images of collagenous (COL, red) and non-collagenous protein deposition by DP cells (NCOL, green) and the **(d-e)** respective quantification showing a reduced secretion by CM-treated DP cells. The same tendency was observed for **(f)** COL/NCOL proteins ratio by ($n = 6$). **(g)** Expression of collagen type-I and fibronectin showing a dimmed signal in the condition where DP cells were treated with KCs-CM. **(h)** Amount of sulfated GAGs showing a reduced production by DP cells cultured with KCs-CM ($n = 4$) as well as different **(i)** deposition pattern of carboxylated and sulfated GAGs in relation to controls. Data shown are mean \pm s.e.m. * $p < 0.05$; ** $p < 0.01$; **** $p < 0.0001$. Scale bars are 50 μ m for **(b,g)**, 100 μ m for **(c)** and 200 μ m for **(i)**. (For interpretation of the references to colour in this figure legend, the reader is referred to the web version of this article.)

Preculture with KCs-CM further aids in the recovery of DP cell phenotype

The artificial promotion of DP cell aggregation in spheroids is so far the gold standard strategy to partially recover human DP phenotype, characterized by low cellular proliferation and increased ALP activity [5,38]. Thus, we prepared 3D spheroids from DP cells precultured in KCs-CM to understand if the features acquired by DP cells cultured in 2D with KCs-CM were retained upon its removal and were comparable to the current gold-standard. In this 3D environment, spheroids formed from DP cells precultured in KCs-CM displayed significantly lower DNA content than controls (Fig. 3a), which is indicative of a low proliferative state, further confirmed by the reduced number of Ki67-positive cells (Fig. 3d). Additionally, preconditioned DP cells maintained the high levels of active ALP (Fig. 3b,e), while the controls showed a small recovery in comparison to the respective 2D cultures (Fig. 3b vs Fig. 1a). A marked decrease in α -SMA expression (Fig. 3f) was also observed, as previously demonstrated in DP-spheroidal cultures [5]. Interestingly, the protein content of spheroids derived from DP cells precultured with KCs-CM was significantly higher than in the respective 3D cultured controls (Fig. 3c). Independently of the pre-culture condition, an ECM composed mostly of fibronectin, collagen I and versican V1 (Fig. 3g-i), and a modest amount of the

V2-isoform of versican (Fig. 3j) involved the tightly connected connexin 43 positive DP cells in the spheroids (Fig. 3k).

Our results show that in 3D spheroids, DP cells precultured in KCs-CM retain the phenotypic features that are associated to an inductive phenotype, which seems to contribute to the improved recovery of DP signature in comparison to the conventional method.

Induction of HF- and SG-like structures in mice

Six weeks after co-grafting DP cells precultured with KCs-CM together with KCs, we observed the formation of HF- and SG-like structures within the wound area of five out of seven animals (Fig. 4a). The reformation of a hair bulb (Fig. 4b, dashed circle, Supplementary Fig. 2a,b) and shaft elongation (Fig. 4b, black arrows) were observed in one animal. From the seven animals where the same DP cells were grafted alone, four showed rudimentary structures (Fig. 4c, Supplementary Fig. 2c), clearly in inferior number and complexity than the ones observed in the co-grafting group. Three animals did not show any structures (Supplementary Fig. 2d), like in control animals (Fig. 4d). The structures found in the experimental group presented a follicular arrangement with multiple epithelial layers, including the presence of a differentiated core layer and some morphologically akin to the hair shaft (Fig. 4e, arrowheads). The follicular nature of these layered structures

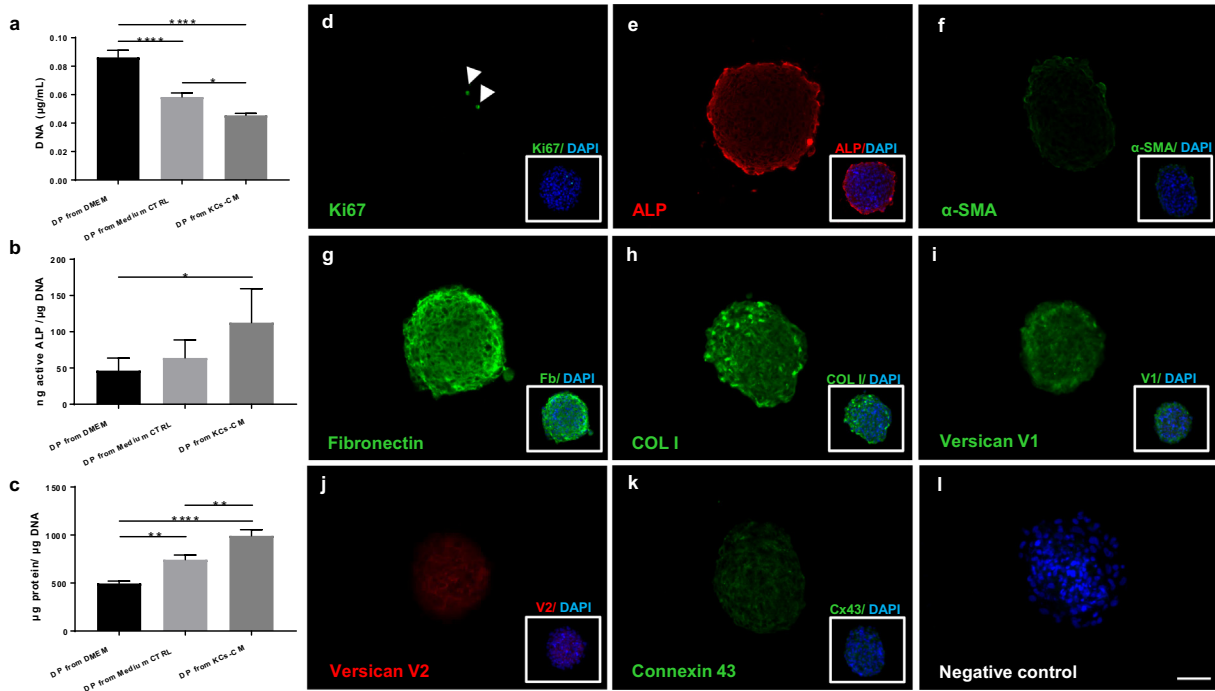


Fig. 3. Preconditioning with KCs-CM further enhances DP signature recovery in 3D culture conditions. DP spheroids derived from cells previously cultured with KCs-CM had a significantly **(a)** lower DNA content, **(b)** higher amount of active ALP and **(c)** higher protein content ($n = 3$). Immunolabelling of DP spheroids preconditioned with KCs-CM showing **(d)** the proliferation-associated marker Ki67 (arrowheads) and the expression of **(e)** ALP, **(f)** α -SMA, **(g)** fibronectin, **(h)** collagen type I, **(i)** V1-isoform of versican, **(j)** V2-isoform of versican and the **(k)** gap junction protein connexin 43. Negative control is depicted on **(l)** and DAPI was used as the nuclear counterstaining (merged images, boxes). Data shown are mean \pm s.e.m. * $p < 0.05$; ** $p < 0.01$; **** $p < 0.0001$. Scale bars = 50 μ m.

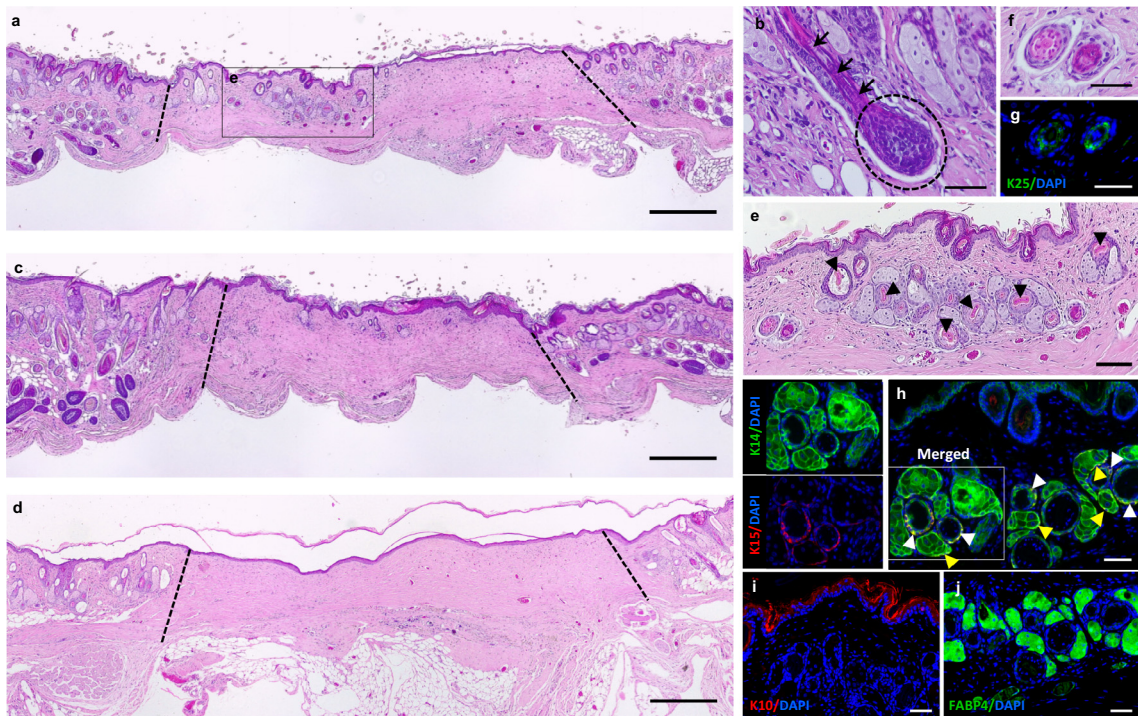


Fig. 4. DP cells preconditioning promotes hair induction in mice. **(a)** H&E staining of the wound sites showing the formation of structures morphologically resembling HF and SGs 6 weeks after grafting CM-precultured DP cells and KCs in immune-deficient mice. **(b)** Hair bulb formation (dashed circle) and hair shaft elongation (arrows) were observed in one of the seven co-grafted animals. **(c)** DP cells grafted alone led to the formation of less complex and less abundant structures which **(d)** were not observed in controls (dotted lines limit the wound area). **(e)** High magnification image of the recreated structures of the experimental condition demonstrating their complexity, including the presence of a differentiated core morphologically alike to hair shafts (arrowheads). **(f)** The folliculoid structures featured distinct epithelial layers, including **(g)** one layer expressing the IRS marker K25, **(h)** a layer co-expressing both K15 and K14 or layers only positive for K14. Arrowheads indicate K14 and K15 co-expression in HF-like (white) and SG-like structure (yellow). **(i)** K10 expression was limited to the skin epithelium, whereas **(j)** the sebocyte marker FABP4 was expressed in the structures resembling SG. Scale bars are 500 μ m for **(a-c)**, 100 μ m for **(d)** and 50 μ m for **(e-j)**. (For interpretation of the references to colour in this figure legend, the reader is referred to the web version of this article.)

(Fig. 4f) was confirmed by the expression of K25, an IRS-specific marker [39] (Fig. 4g), and K15 and K14, linked to the hair bulge and ORS. Proliferative areas co-expressing K14 and K15 (Fig. 4h), as observed in the hair bulge and the immature portions of the ORS, were also identified. Due to the immature nature of the observed structures, K10 staining was only observed in the outermost layers of the skin (Fig. 4i). Furthermore, analysis of the wound area evidenced the presence of blood vessels surrounding the structures (Supplementary Fig. 2e, arrowheads). The presence of sebocytes into the SG-like structures was confirmed by FABP4 expression (Fig. 4j). While human cells were not identified as part of the recreated follicular and SG-like structures, they were occasionally identified within the dermis of some animals where DP cells were grafted alone and no structures were formed (Supplementary Fig. 3).

Discussion

Unlike their rodent counterparts, human DP cells suffer a dramatic loss of their inductive abilities when cultured *in vitro* and do not naturally recover from it when implanted *in vivo* [40]. The loss of contextual microenvironmental cues, especially from the surrounding epithelial cells and the paracrine signalling molecules they provide, is commonly appointed as a causing event for this phenomenon [4,41]. Considering this, we took advantage of the KCs secretome to rescue DP cell intrinsic properties in culture, therefore enabling their propagation and use for human cell-based HF regenerative approaches.

Cultivation with KCs-CM markedly increased ALP activity in DP cells, a critical hair inductive marker [42]. It also improved DP cell self-aggregative capacity, a distinctive behaviour that correlates with their hair induction ability [38,40,43]. Interestingly, when CM-precultured DP cells were used to form 3D spheroids, the current gold-standard method to restore human DP signature [4,5], ALP activity was maintained. This is in line with the modest increase observed also in the conventional 3D spheroid cultures, suggesting that KCs-CM may be a stronger stimulus to restore this phenotypic marker. Furthermore, culture with KCs-CM significantly decreased α -SMA and versican V1 expression, better resembling the native phenotype of DP cells, where these markers are absent or expressed in low levels [21,22], respectively. The low expression of α -SMA expression was kept in spheroids, similarly to what was previously described for DP cells [5,44]. Moreover, CM pretreated DP cells secreted lower amounts of ECM proteins when cultured in 2D conditions. Some authors defend that without contextual and positional signals, DP cells suffer de-differentiation [41] in 2D cultures and behave like dermal fibroblasts, whose main function in skin is to synthesize and maintain the ECM. Indeed, 2D cultured DP cells are highly effective in replacing dermal fibroblasts in the establishment of the dermal component of engineered skin [45], which further supports those observations. Therefore, the decreased ECM production observed for 2D cultured DP cells in the presence of KCs-CM may indicate prevention of that de-differentiation event, especially when associated with increased ALP activity.

Since DP control over HF development and hair growth is based in a well-controlled network of bioactive molecules, the use of human DP cells in HF-regenerative strategies will strongly rely on their capacity to respond in a physiologically relevant manner. Under KCs-CM influence, DP cells produced significantly more VEGF, whereas BMP and TGF- β 1 signalling were downregulated, which coincide with what has been reported to be necessary for hair induction [26,30,46]. The most impressive effect of KCs-CM was, however, the remarkable increase in IL-6 secretion. Literature concerning the effects of IL-6 in HF regulation is scant, however, IL-6 expression has been shown to be higher in the anagen HF in

comparison to non-follicular skin [27]. Moreover, Tanabe *et al* [47] showed that daily injections of 200 ng (1 μ g/mL) of IL-6 or higher promoted hair growth in rats. On the other hand, Huang and co-workers [48] reported an inhibitory effect of lower doses of IL-6 (250–500 pg/mL) on KCs growth, which seems to indicate a specific dose-dependent effect. Therefore, the dramatic increase of IL-6 secretion that we observed when DP cells were cultured with KCs-CM might be an additional beneficial feature to recover hair inductive phenotype. Taken together, our results demonstrate that after culture with KCs-CM the secretome profile of DP cells matches the one characteristic of the anagen phase.

Despite the encouraging evidence observed *in vitro*, the demonstration of KCs-CM capacity to support DP cell hair-inductive ability ultimately relies on *in vivo* cellular engraftment. We showed that DP cells precultured with KCs-CM, and combined with adult KCs, were able to induce the formation of follicular structures that recreated the main features of HFs and SG. Although hair bulb reformation occurred in one of the animals, the presence and elongation of hair fibres were not observed in the majority, demonstrating the immature state of the regenerated structures. Our approach takes advantage of human-epithelial signalling to improve DP cell inductivity, but there are other cellular players involved in hair growth whose lack and/or substantial interspecies differences may have prevented complete HF formation. Nevertheless, as far as we know, this represents the best result obtained so far using entirely adult human cells, both DP cells and KCs, for HF regeneration. Previously, Ehama *et al.* [49] demonstrated the formation of chimeric HFs using murine DP cells and human neonatal KCs, but the combination of both human-origin cells did not show any sign of follicular generation. Later, the combination of cultured human KCs and DP cells led to the formation of what seem to be epithelial structures adjacent to the skin epidermis, but their multicellular epithelial composition was not confirmed and the formation of SG was not observed [50]. We also observed the presence of small vessels around the structures, a functional indicator since a follicular and perifollicular vasculature network is intimately coupled with hair growth [26,51,52]. *In vitro* results demonstrate that KCs produce VEGF and that their CM boosted VEGF production by DP cells, therefore both cells may have contributed to the establishment and localization of the observed microvasculature *in vivo*. Remarkably, HF- and SG-like structures were also spotted in most animals where preconditioned DP cells were grafted alone, although their complexity and occurrence were clearly inferior to the ones observed in co-grafted animals. Having in consideration previous works showing that DP cells alone do not induce hair formation [49,50], those results further suggest that KCs-CM improve the inductive ability of DP cells, which could induce the host epithelium into a follicular or SG fate.

The absence of human cells within the recreated structures after 6 weeks, might be related to the model used, in which cells are not grafted subcutaneously but in the inflicted wound. The chamber assay is characterized by continuous tissue remodelling lead by the wound healing environment, therefore, we can speculate that grafted cells were replaced along the time. In fact, cellular interchangeability and interspecies cooperation leading to grafted epithelial cells replacement by host KCs was previously reported in the same model [49]. This is also in line with another work showing that human cells detected both in the epidermis and in folliculoid structures formed after rabbit DP cells induction, were completely replaced within one month [53].

As hypothesised, and based on previous results demonstrating KCs-CM mitogenic effect over DP cells [8,13], with our strategy we were able to restore DP cell phenotype and inductive properties, while supporting their growth in culture. The increase in the proliferative capacity of 2D cultured DP cells was most likely due to the presence of PDGF-A and VEGF in KCs-CM, both known

mitogenic factors for DP cells [25,54]. Still, spheroids inclosing DP cells precultured with KCs-CM displayed lower proliferative capacity in comparison to conventionally produced spheroids, demonstrating an improved capacity to recreate the DP quiescent state *in situ* and the importance of different culture conditions (2D vs 3D).

To conclude, our observations demonstrate that CM collected from adult interfollicular KCs represents an effective strategy to improve key human DP cell native features *in vitro*, including their critical inductivity and self-aggregation capacity. Further, KCs-CM improved DP cell proliferation and the secretion profile of known paracrine mediators of hair growth, better ensuring that a sufficient number of functional cells are obtained. Finally, *in vivo* testing of CM-precultured DP cells demonstrated their capacity to support the recreation of HF- and SG-like structures, especially in combination with KCs. We believe that the high translational value of our strategy and its easy application hold great promise for supporting upcoming advances in the hair regenerative field.

Author contributions

C. M. Abreu performed the majority of the experiments and the correspondent data analysis, generated final figures, and wrote the manuscript. M. T. Cerqueira established J2-3T3 fibroblasts and KCs cultures at 3B's Research Group, performed flow cytometry assays and correspondent data analysis, discussed the data and reviewed the manuscript. R. P. Pirraco collaborated in the *in vivo* experiment, discussed the data and reviewed the manuscript. L. Gasperini performed the CellProfiler™ analysis and assisted during the correspondent data analysis. R. L. Reis secured research funding and resources availability. A. P. Marques is responsible for the conception and design of the study, raised funds and managed the project, interpreted overall data and reviewed the final manuscript.

Compliance with Ethics Requirements

All Institutional and National Guidelines for the care and use of animals (fisheries) were followed.

Declaration of Competing Interest

The authors declare that they have no known competing financial interests or personal relationships that could have appeared to influence the work reported in this paper.

Acknowledgements

The research reported in this publication was supported by FCT/MCTES (Fundação para a Ciência e a Tecnologia/ Ministério da Ciência, Tecnologia, e Ensino Superior) through the PD/59/2013, PD/BD/113800/2015 (C. Abreu), CEECIND/00695/2017 (M. T. Cerqueira), IF/00347/2015 (R. Pirraco), IF/00945/2014 (A. P. Marques) and UIDB/50026/2020 grants. We thank Manuela Lago for her support on experimental assays and to Emanuel Rognoni and Simon Broad from King's College London for their expert technical assistance in the establishment of the *in vivo* chamber model in our group.

Appendix A. Supplementary data

Supplementary data to this article can be found online at <https://doi.org/10.1016/j.jare.2020.10.006>.

References

- [1] Yang C-C, Cotsarelis G. Review of hair follicle dermal cells. *J. Dermatol. Sci.* 2010;57:2–11. doi: <https://doi.org/10.1016/j.jdermsci.2009.11.005>.
- [2] Driskell RR, Clavel C, Rendl M, Watt FM. Hair follicle dermal papilla cells at a glance. *J. Cell Sci.* 2011;124:1179–82. doi: <https://doi.org/10.1242/jcs.082446>.
- [3] Ohyama M, Zheng Y, Paus R, Stenn KS. The mesenchymal component of hair follicle neogenesis: background, methods and molecular characterization. *Exp. Dermatol.* 2010;19:89–99. doi: <https://doi.org/10.1111/j.1600-0625.2009.00935.x>.
- [4] Higgins CA, Chen JC, Cerise JE, Jahoda CAB, Christiano AM. Microenvironmental reprogramming by three-dimensional culture enables dermal papilla cells to induce de novo human hair-follicle growth. *Proc. Natl. Acad. Sci.* 2013;110:19679–88. doi: <https://doi.org/10.1073/pnas.1309970110>.
- [5] Higgins CA, Richardson GD, Ferdinando D, Westgate GE, Jahoda CAB. Modelling the hair follicle dermal papilla using spheroid cell cultures. *Exp. Dermatol.* 2010;19:546–8. doi: <https://doi.org/10.1111/j.1600-0625.2009.01007.x>.
- [6] Yamauchi K, Kurosaka A. Inhibition of glycogen synthase kinase-3 enhances the expression of alkaline phosphatase and insulin-like growth factor-1 in human primary dermal papilla cell culture and maintains mouse hair bulbs in organ culture. *Arch. Dermatol. Res.* 2009;301:357–65. doi: <https://doi.org/10.1007/s00403-009-0929-7>.
- [7] Ohyama M, Kobayashi T, Sasaki T, Shimizu A, Amagai M. Restoration of the intrinsic properties of human dermal papilla *in vitro*. *J. Cell Sci.* 2012;125:4114–25. doi: <https://doi.org/10.1242/jcs.105700>.
- [8] Won CH, Jeong YM, Kang S, Koo TS, Park SH, Park KY, et al. Hair-growth-promoting effect of conditioned medium of high integrin $\alpha 6$ and low CD 71 ($\alpha 6$ bri/CD71dim) positive keratinocyte cells. *Int. J. Mol. Sci.* 2015;16:4379–91. doi: <https://doi.org/10.3390/ijms16034379>.
- [9] Sennett R, Rendl M. Mesenchymal–epithelial interactions during hair follicle morphogenesis and cycling. *Semin. Cell Dev. Biol.* 2012;23:917–27. doi: <https://doi.org/10.1016/j.semcdb.2012.08.011>.
- [10] Roh C, Tao Q, Lyle S. Dermal papilla-induced hair differentiation of adult epithelial stem cells from human skin. *Physiol. Genomics.* 2005;19:207–17. doi: <https://doi.org/10.1152/physiolgenomics.00134.2004>.
- [11] Bak SS, Kwack MH, Shin HS, Kim JC, Kim MK, Sung YK. Restoration of hair-inductive activity of cultured human follicular keratinocytes by co-culturing with dermal papilla cells. *Biochem. Biophys. Res. Commun.* 2018;505:360–4. doi: <https://doi.org/10.1016/j.bbrc.2018.09.125>.
- [12] Limat A, Hunziker T, Waelti ER, Inaebnit SP, Wiesmann U, Braathen LR. Soluble factors from human hair papilla cells and dermal fibroblasts dramatically increase the clonal growth of outer root sheath cells. *Arch. Dermatol. Res.* 1993;285:205–10. doi: <https://doi.org/10.1007/BF00372010>.
- [13] Warren R, Wong TK. Stimulation of human scalp papilla cells by epithelial cells. *Arch. Dermatol. Res.* 1994;286:1–5. doi: <https://doi.org/10.1007/BF00375835>.
- [14] Cerqueira MT, Frias AM, Reis RL, Marques AP. Boosting and Rescuing Epidermal Superior Population from Fresh Keratinocyte Cultures. *Stem Cells Dev.* 2014;23:34–43. doi: <https://doi.org/10.1089/scd.2013.0038>.
- [15] K. Gledhill, A. Gardner, C.A.B. Jahoda, Isolation and Establishment of Hair Follicle Dermal Papilla Cell Cultures, in: *Methods Mol. Biol., Methods Mol Biol*, 2013; pp. 285–292.
- [16] López-De León A, Rojkind M. A simple micromethod for collagen and total protein determination in formalin-fixed paraffin-embedded sections. *J. Histochem. Cytochem.* 1985;33:737–43. doi: <https://doi.org/10.1177/33.8.2410480>.
- [17] Kafienah W, Sims TJ. *Biochemical Methods for the Analysis of Tissue-Engineered Cartilage*, in: *Methods Tissue Eng. New Jersey: Humana Press; 2003. p. 217–30.*
- [18] Lamprecht MR, Sabatini DM, Carpenter AE. Cell Profile™: free, versatile software for automated biological image analysis. *Biotechniques* 2007;42:71–5. doi: <https://doi.org/10.2144/000112257>.
- [19] Sankur B. Survey over image thresholding techniques and quantitative performance evaluation. *J. Electron. Imaging.* 2004;13:146. doi: <https://doi.org/10.1117/1.1631315>.
- [20] Jensen KB, Driskell RR, Watt FM. Assaying proliferation and differentiation capacity of stem cells using disaggregated adult mouse epidermis. *Nat. Protoc.* 2010;5:898–911. doi: <https://doi.org/10.1038/nprot.2010.39>.
- [21] C.A.B. Jahoda, A.J. Reynolds, C. Chaponnier, J.C. Forester, G. Gabbiani. Smooth muscle alpha-actin is a marker for hair follicle dermis *in vivo* and *in vitro*. *J. Cell Sci.* 99 (Pt 3) (1991) 627–36.
- [22] Soma T, Tajima M, Kishimoto J. Hair cycle-specific expression of versican in human hair follicles. *J. Dermatol. Sci.* 2005;39:147–54. doi: <https://doi.org/10.1016/j.jdermsci.2005.03.010>.
- [23] Iida M, Ihara S, Matsuzaki T. Hair cycle-dependent changes of alkaline phosphatase activity in the mesenchyme and epithelium in mouse vibrissal follicles. *Dev. Growth Differ.* 2007;49:185–95. doi: <https://doi.org/10.1111/j.1440-169X.2007.00907.x>.
- [24] Mecklenburg L, Tobin DJ, Müller-Röver S, Handjiski B, Wendt G, Peters EMJ, et al. Active Hair Growth (Anagen) is Associated with Angiogenesis. *J. Invest. Dermatol.* 2000;114:909–16. doi: <https://doi.org/10.1046/j.1523-1747.2000.00954.x>.
- [25] Lachgar S, Moukadiri H, Jonca F, Charveron M, Bouhaddiou N, Gall Y, et al. Vascular Endothelial Growth Factor Is an Autocrine Growth Factor for Hair

- Dermal Papilla Cells. *J. Invest. Dermatol.* 1996;106:17–23. doi: <https://doi.org/10.1111/1523-1747.ep12326964>.
- [26] Yano K, Brown LF, Detmar M. Control of hair growth and follicle size by VEGF-mediated angiogenesis. *J. Clin. Invest.* 2001;107:409–17. doi: <https://doi.org/10.1172/JCI11317>.
- [27] M. Yu, S. Kissling, P. Freyschmidt-Paul, R. Hoffmann, J. Shapiro, K.J. McElwee, Interleukin-6 cytokine family member oncostatin M is a hair-follicle-expressed factor with hair growth inhibitory properties. *Exp. Dermatol.* 17 (2007) 071117031607006-???. <https://doi.org/10.1111/j.1600-0625.2007.00643.x>.
- [28] Taniguchi K, Arima K, Masuoka M, Ohta S, Shiraishi H, Ontsuka K, et al. Periostin controls keratinocyte proliferation and differentiation by interacting with the paracrine IL-1 α /IL-6 loop. *J. Invest. Dermatol.* 2014;134:1295–304. doi: <https://doi.org/10.1038/jid.2013.500>.
- [29] Botchkarev VA, Botchkareva NV, Roth W, Nakamura M, Chen L-H, Herzog W, et al. Noggin is a mesenchymally derived stimulator of hair-follicle induction. *Nat. Cell Biol.* 1999;1:158–64. doi: <https://doi.org/10.1038/11078>.
- [30] Foitzik K, Lindner G, Mueller-Roever S, Maurer M, Botchkareva N, Botchkarev V, et al. Control of murine hair follicle regression (catagen) by TGF- β 1 in vivo. *FASEB J.* 2000;14:752–60. doi: <https://doi.org/10.1096/fasebj.14.5.752>.
- [31] Tomita Y, Akiyama M, Shimizu H. PDGF isoforms induce and maintain anagen phase of murine hair follicles. *J. Dermatol. Sci.* 2006;43:105–15. doi: <https://doi.org/10.1016/j.jiddermsci.2006.03.012>.
- [32] Festa E, Fretz J, Berry R, Schmidt B, Rodeheffer M, Horowitz M, et al. Adipocyte lineage cells contribute to the skin stem cell niche to drive hair cycling. *Cell* 2011;146:761–71. doi: <https://doi.org/10.1016/j.cell.2011.07.019>.
- [33] Tobin DJ, Gunin A, Magerl M, Handijski B, Paus R. Plasticity and cytokinetic dynamics of the hair follicle mesenchyme: Implications for hair growth control. *J. Invest. Dermatol.* 2003;120:895–904. doi: <https://doi.org/10.1046/j.1523-1747.2003.12237.x>.
- [34] Messenger AG. Isolation, culture and in vitro behavior of cells isolated from papillae of human hair follicles. In: *Trends Hum. Hair Growth Alopecia Res.* Netherlands: Springer; 1989. p. 57–66.
- [35] Upton JH, Hannen RF, Bahta AW, Farjo N, Farjo B, Philpott MP. Oxidative Stress-Associated Senescence in Dermal Papilla Cells of Men with Androgenetic Alopecia. *J. Invest. Dermatol.* 2015;135:1244–52. doi: <https://doi.org/10.1038/jid.2015.28>.
- [36] Couchman JR. Rat Hair Follicle Dermal Papillae Have an Extracellular Matrix Containing Basement Membrane Components. *J. Invest. Dermatol.* 1986;87:762–7. doi: <https://doi.org/10.1111/1523-1747.ep12456955>.
- [37] Messenger AG, Elliott K, Westgate GE, Gibson WT. Distribution of extracellular matrix molecules in human hair follicles. *Ann. N. Y. Acad. Sci.* 1991;642:253–62. doi: <https://doi.org/10.1111/j.1749-6632.1991.tb24392.x>.
- [38] Young T-H, Lee C-Y, Chiu H-C, Hsu C-J, Lin S-J. Self-assembly of dermal papilla cells into inductive spheroidal microtissues on poly(ethylene-co-vinyl alcohol) membranes for hair follicle regeneration. *Biomaterials* 2008;29:3521–30. doi: <https://doi.org/10.1016/j.biomaterials.2008.05.013>.
- [39] Schweizer J, Langbein L, Rogers MA, Winter H. Hair follicle-specific keratins and their diseases. *Exp. Cell Res.* 2007;313:2010–20. doi: <https://doi.org/10.1016/j.yexcr.2007.02.032>.
- [40] Jahoda CAB, Oliver RF. Vibrissa dermal papilla cell aggregative behaviour in vivo and in vitro. *J. Embryol. Exp. Morphol.* 1984;79:211–24.
- [41] Ramos R, Guerrero-Juarez CF, Plikus MV. Hair Follicle Signaling Networks: A Dermal Papilla-Centric Approach. *J. Invest. Dermatol.* 2013;133:2306–8. doi: <https://doi.org/10.1038/jid.2013.262>.
- [42] McElwee KJ, Kissling S, Wenzel E, Huth A, Hoffmann R. Cultured peribulbar dermal sheath cells can induce hair follicle development and contribute to the dermal sheath and dermal papilla. *J. Invest. Dermatol.* 2003;121:1267–75. doi: <https://doi.org/10.1111/j.1523-1747.2003.12568.x>.
- [43] Nilforoushadeh MA, Zare M, Zarrintaj P, Alizadeh E, Taghiabadi E, Heidari-Kharaji M, et al. Engineering the niche for hair regeneration – A critical review, Nanomedicine Nanotechnology. *Biol. Med.* 2019. doi: <https://doi.org/10.1016/j.nano.2018.08.012>.
- [44] Gupta AC, Chawla S, Hegde A, Singh D, Bandyopadhyay B, Lakshmanan CC, et al. Establishment of an in vitro organoid model of dermal papilla of human hair follicle. *J. Cell. Physiol.* 2018;233:9015–30. doi: <https://doi.org/10.1002/jcp.26853>.
- [45] Higgins CA, Roger MF, Hill RP, Ali-Khan AS, Garlick JA, Christiano AM, et al. Multifaceted role of hair follicle dermal cells in bioengineered skins. *Br. J. Dermatol.* 2017;176:1259–69. doi: <https://doi.org/10.1111/bjd.15087>.
- [46] Botchkarev VA, Botchkareva NV, Nakamura M, Huber O, Funa K, Lauster R, et al. Noggin is required for induction of the hair follicle growth phase in postnatal skin. *FASEB J.* 2001;15:2205–14. doi: <https://doi.org/10.1096/fj.01-0207com>.
- [47] Tanabe A, Ogawa Y, Takemoto T, Wang Y, Furukawa T, Kono H, et al. Interleukin 6 induces the hair follicle growth phase (anagen). *J. Dermatol. Sci.* 2006;43:210–3. doi: <https://doi.org/10.1016/j.jiddermsci.2006.04.004>.
- [48] Huang W-Y, Huang Y-C, Huang K-S, Chan C-C, Chiu H-Y, Tsai R-Y, et al. Stress-induced premature senescence of dermal papilla cells compromises hair follicle epithelial-mesenchymal interaction. *J. Dermatol. Sci.* 2017;86:114–22. doi: <https://doi.org/10.1016/j.jiddermsci.2017.01.003>.
- [49] Ehama R, Ishimatsu-Tsuji Y, Iriyama S, Ideta R, Soma T, Yano K, et al. Hair Follicle Regeneration Using Grafted Rodent and Human Cells. *J. Invest. Dermatol.* 2007;127:2106–15. doi: <https://doi.org/10.1038/sj.jid.5700823>.
- [50] Inoue K, Kato H, Sato T, Osada A, Aoi N, Suga H, et al. Evaluation of Animal Models for the Hair-Inducing Capacity of Cultured Human Dermal Papilla Cells. *Cells Tissues Organs.* 2009;190:102–10. doi: <https://doi.org/10.1159/000178021>.
- [51] Lachgar Charveron, Gall Bonafe. Minoxidil upregulates the expression of vascular endothelial growth factor in human hair dermal papilla cells. *Br. J. Dermatol.* 1998;138:407–11. doi: <https://doi.org/10.1046/j.1365-2133.1998.02115.x>.
- [52] Chew EGY, Tan JHJ, Bahta AW, Ho BS-Y, Liu X, Lim TC, et al. Differential Expression between Human Dermal Papilla Cells from Balding and Non-Balding Scalps Reveals New Candidate Genes for Androgenetic Alopecia. *J. Invest. Dermatol.* 2016;136:1559–67. doi: <https://doi.org/10.1016/j.jid.2016.03.032>.
- [53] Ferraris C, Bernard BA, Dhouailly D. Adult epidermal keratinocytes are endowed with pilosebaceous forming abilities. *Int. J. Dev. Biol.* 1997;41:491–8. doi: <https://doi.org/10.1387/ijdb.9240566>.
- [54] Karlsson L, Bondjers C, Betsholtz C. Roles for PDGF-A and sonic hedgehog in development of mesenchymal components of the hair follicle. *Development.* 1999;126:2611–21.